Equation of State of Hypermatter in β Equilibrium in a Quark Model with Excluded Volume Correction *

R. M. Aguirre and A. L. De Paoli.
Departamento de Física, Fac. de Ciencias Exactas,
Universidad Nacional de La Plata.
C. C. 67 (1900) La Plata, Argentina.

February 7, 2008

Abstract

We study the effects of the finite size of the baryons on the equation of state of homogeneous hadronic matter with hyperons. The finite extension of hadrons is introduced in order to improve the perfomance of field theoretical models at very high densities, simulating the short-range hard-core repulsive part of the baryon-baryon potential. We choose the Quark Meson Coupling model to describe the baryon dynamics because this model provides a density dependent radius of the bag. In addition we calculate finite size corrections for the Zimanyi-Moszkowski model in order to make a definite comparison. In both cases finite size effects are implemented through a Van der Waals like correction in the normalization of the baryon fields. In this approach we investigate β-stable matter in conditions that could be found in the interior of massive stars. We find that the excluded volume corrections contribute significantly for densities above twice the symmetric nuclear matter saturation density, although for the quark model the results strongly depends upon the equilibrium conditions for the confinement volume immersed in a dense medium.

PACS : 12.39.Ba, 13.75.Ev, 21.30.Fe, 21.65.+f, 26.60.+c

* *This work was partially supported by the project PMT-PICT0079 of ANPCYT, (FONCYT) Argentina.*

1 Introduction

Investigation of hadronic matter in extreme conditions of density and temperature is of relevance in physics since the knowledgwe of its properties will eventually lead to clarify some questions about fundamental interactions and the recovering of QCD symmetries [1, 2].

The role of strangeness in the evolution of relativistic heavy-ion collisions [3] as well as in the dynamics of neutron stars [4] has been stated long time ago. Near the surface of a neutron star, where the density is of the order of the normal nuclear density n_0, hadronic matter is mainly composed by protons and neutrons in β equilibrium with electrons, in such a way that the whole system remains electrically neutral. At higher densities (2-3 n_0) hyperons could appear, decreasing the energy per baryon. Further increasing of the density could cause the formation of different exotic phases composed of mesons condensates, quark matter lumps or quark-gluon plasma. The transition among phases are esentially pressure induced, and differs qualitatively when there are one or two conserved charges, *e.g.* baryon number and electric charge [5].

In most hadronic matter studies, the interacting particles are assumed as point-like. In an early work [6], it was claimed the necessity to take care of the spatial extension of the hadrons and the influence of this fact on the collective phenomena at very high densities. It is worthy to mention that there are only a few field theoretical models which consistently includes the dynamics of the hadron volume, the most commonly used are the Skyrme and bag-like models. In the first case the inclusion of finite baryon density effects is not straightforward due to the topological character of its solutions [7]. On the other hand further refinements of the original MIT bag model allows to deal with medium effects upon the hadron structure [8]-[10]. Also in a recent work [10], attempts to include repulsion between overlapping bags was done through effective short-range quark-quark correlations.

Even when finite size hadrons are considered, the associated hard core repulsion among baryons in the nuclear medium is frequently not taken into account. At densities lower than n_0 finite volume effects are small, but these repulsive corrections could be very important at higher densities. For the case of hyperon matter, this fact affects the relative population of the different baryonic components.

The main difficulty to deal with a hard core potential is that it does not admit a perturbative treatment at high densities. Hence it would be desirable to have an effective treatment of these volume effects without leaving the simplicity of the quasiparticle approximation.

We adopt a Van der Waals-like method to take into account finite volume corrections. In this scheme the total volume appearing in the thermodynamical quantities is replaced by the available volume, therefore it has the advantage that the volume of the particle is the only new parameter introduced to represent the hard core repulsive correlations. A similar approach has been used in related investigations, as for instance in references [11]-[15].

In the present work we want to generalize the excluded volume corrections to study the properties of hadron matter with strangeness, and to check out to what extent the usual nuclear field effective models can be used to

extrapolate the hypermatter equation of state at high densities. We introduce these corrections at the level of the normalization of the baryon fields. This point of view allows us to use the same effective Lagrangians usually applied to describe the dynamics of point-like particles. Therefore in the quasi-particle scheme of the Mean Field Approximation for homogeneous matter, the baryons as a whole will be described by a superposition of relativistic plane waves, but they will move only within the accessible volume.

We shall apply this approach to study the properties of homogeneous hypermatter in β-equilibrium at zero temperature. Although the formalism is stated for the whole baryon octet, in order to clarify the discussions we shall only consider Λ hyperons in our calculations, besides neutrons and protons. The equation of state of nuclear matter with lambdas has been previously investigated in non-relativistic [17] as well as for relativistic [18] regimes considering point-like particles. However a full treatment must include heavier hyperons, as deduced for example, from the influence of the Ξ particles on the stability of lambdas in medium [19].

In the next section we give a resume of the effective models to be used in our calculations. Section 3 is devoted to extend these models to include correlations based in excluded volume restrictions. To compare the effects of the correction proposed, we have selected two descriptions of very different kind. On one hand we select a hadronic Lagrangian for point-like particles, the so-called Zimanyi-Moszkowski (ZM) model [20], for which a fictitious size is assigned to the baryons, and on the other hand we have a bag model generalized to include quarks interacting with scalar and vector mesons, the Quark Meson Coupling (QMC) model [8, 9]. In the last case two possible conditions for the equilibrium of the confinement volume in dense matter are proposed. All these items are discussed in section 4. Numerical results and discussion are given in section 5, conclusions are drawn in section 6.

2 Relativistic Effective Lagrangian for Point-like Baryons

Relativistic Hadron Field Theories have proved to be adequate in describing many nuclear matter properties at saturation density, and also finite nuclei structure, with a relatively small number of free parameters. These theories allow to extrapolate matter behaviour to high densities and energies. Although a chiral treatment is desirable at high densities, we do not consider this issue in this work.

There are a variety of effective relativistic Lagrangians, the more usual ones describe nuclear interaction mediated by scalar (σ), vector (ω) and pseudovector (ρ) mesons [20, 21, 22]. Since neutral matter at high densities can be composed not only by nucleons and leptons but also with more massive baryons, we select a Lagrangian of the form:

$$\begin{aligned}\mathcal{L} &= \sum_B \left[\bar{\Psi}^B(i\gamma^\mu\partial_\mu - g_\omega^B\gamma^\mu\omega_\mu - \frac{1}{2}g_\rho^B\,\gamma^\mu\tau.\mathbf{b}_\mu - {M_B}^*)\Psi^B\right] \\ &+ \frac{1}{2}(\partial^\mu\sigma\partial_\mu\sigma - {m_\sigma}^2\,\sigma^2) - \frac{1}{4}F^{\mu\nu}F_{\mu\nu} + \frac{1}{2}{m_\omega}^2\,\omega^\mu\omega_\mu\end{aligned}$$

$$- \quad \frac{1}{4}\mathbf{G}^{\mu\nu}\mathbf{G}_{\mu\nu} + \frac{1}{2}{m_\rho}^2\ \mathbf{b}^\mu.\mathbf{b}_\mu + \sum_l \left[\bar{\Psi}^l(i\gamma^\mu\partial_\mu - m_l)\Psi^l\right] \qquad (2.1)$$

In Eq.(2.1) $F^{\mu\nu}$ and $\mathbf{G}^{\mu\nu}$ are the tensor strength fields of the ω and ρ mesons, respectively, and the index $B(l)$ runs over all baryons (leptons) considered. The term ${M_B}^*$ contains the interaction of the σ meson with the baryonic fields Ψ^B, and plays the role of the baryon effective mass. The different forms of ${M_B}^*$ lead to a family of hadronic Lagrangians. In order to have a general discussion ${M_B}^*$ will be kept undetermined until needed.
We solve the field equations for the case of homogeneous infinite static matter in the mean field approximation (MFA) [21, 22]. In this case all meson fields are replaced by their average values, i. e.

$$\sigma = \sigma_0 = -\frac{1}{{m_\sigma}^2}\sum_B \frac{d{M_B}^*}{d\sigma} n_s^B \qquad (2.2)$$

$$\omega_\mu = \omega_0\delta_{\mu 0} = \frac{1}{{m_\omega}^2}\sum_B g_\omega^B n^B\ \delta_{\mu 0} \qquad (2.3)$$

$$b_\mu^a = b_0\delta_{\mu 0}\delta_{a3} = \frac{1}{{m_\rho}^2}\sum_B g_\rho^B I_3^B n^B\ \delta_{\mu 0}\delta_{a3} \qquad (2.4)$$

where $a = 1, 2, 3$ runs over all isospin directions and I_3^B is the third isospin component of baryon B. In all our calculations we use the values of $m_\sigma = 550MeV$, $m_\omega = 783MeV$, and $m_\rho = 770MeV$ for the meson masses.
The equation of motion for the baryon field B (spin 1/2) is

$$(i\gamma^\mu\partial_\mu - g_\omega^B\gamma^0\omega_0 - g_\rho^B I_3^B\ \gamma^0 b_0 - {M_B}^*)\Psi^B = 0 \qquad (2.5)$$

The equation above can be used to define the energy k_0 for a baryon carrying momentum $\vec{k}$

$$k_0^B = \sqrt{{M_B}^{*2} + \vec{k}^2} \pm g_\omega^B\omega_0 \pm g_\rho^B I_3^B b_0 \qquad (2.6)$$

for particle (+) and antiparticle (−) solutions. Within the MFA at zero temperature only the particle solutions contributes.
The scalar (n_s^B) and baryonic (n^B) densities are defined with respect to the ground state of the system $|GS>$ for each baryonic class

$$n_s^B =< GS|\bar{\Psi}^B\ \Psi^B|GS >= \vartheta\ \frac{1}{\pi^2}{M_B}^*\int_0^{k_B} dk \frac{k^2}{\sqrt{{M_B}^{*2} + k^2}} \qquad (2.7)$$

$$n^B =< GS|{\Psi^\dagger}^B\Psi^B|GS >= \ \vartheta\ \frac{{k_B}^3}{3\pi^2} \qquad (2.8)$$

In Eqs. (2.7) and (2.8) k_B is the Fermi momentum for baryons and the factor $\vartheta = 1$ for point-like baryons.

For the Lagrangian (2.1) leptons behaves like free Dirac particles. The leptonic density n_l defines the Fermi momentum k_l through

$$n^l =< GS|{\Psi^\dagger}^l\Psi^l|GS >= \frac{{k_l}^3}{3\pi^2} \qquad (2.9)$$

Mean field equations are solved for fixed total baryon density n and zero total electric density charge n^e:

$$\begin{aligned} n &= \sum_B n^B \qquad (2.10) \\ n^e &= \sum_B q^B n^B + \sum_l q^l n^l = 0 \qquad (2.11) \end{aligned}$$

where q^B are the baryon electric charges, $q^l = -e$ the electron and muon charges.
All baryon and lepton species are assumed to be in β equilibrium. This constraint and the condition (2.11) determine the relative population of the particles. In the present work we consider only three baryon species, namely $B =$ proton (p), neutron (n), lambda (Λ), and two lepton species, $l =$ electron (e), muon (μ).
Consequently chemical equilibrium is impossed through the following relationships among the chemical potentials μ:

$$\begin{aligned} \mu^n &= \mu^p + \mu^e \\ \mu^n &= \mu^\Lambda, \quad \text{(if lambdas are present)} \\ \mu^e &= \mu^\mu, \quad \text{(if muons are present)} \qquad (2.12) \end{aligned}$$

with $\mu^B = k_0^B(k_B)$, see Eq. (2.6), and $\mu^l = k_0^l(k_l) = \sqrt{{m_l}^2 + {k_l}^2}$.
One solves the system of equations (2.2) to (2.12) for a fixed value of the total baryon density. This determines the meson fields $(\sigma_0, \omega_0, b_0)$, the baryon and lepton densities (n^B, n^l), all the Fermi momenta (k_B, k_l) and chemical potentials (μ^B, μ^l).
Once the solution has been found, we can calculate the total energy density

$$\begin{aligned} \epsilon &= \frac{1}{2}{m_\sigma}^2\ {\sigma_0}^2 + \frac{1}{2}{m_\omega}^2\ {\omega_0}^2 + \frac{1}{2}{m_\rho}^2\ {b_0}^2 \\ &+ \frac{\vartheta}{\pi^2}\sum_B \int_0^{k_B} dk k^2 \sqrt{{M_B^*}^2 + k^2} \\ &+ \frac{1}{\pi^2}\sum_l \int_0^{k_l} dk k^2 \sqrt{{m_l}^2 + k^2} \qquad (2.13) \end{aligned}$$

and the total pressure

$$\begin{aligned} p &= -\frac{1}{2}{m_\sigma}^2\ {\sigma_0}^2 + \frac{1}{2}{m_\omega}^2\ {\omega_0}^2 + \frac{1}{2}{m_\rho}^2\ {b_0}^2 \\ &+ \frac{\vartheta}{3\pi^2}\sum_B \int_0^{k_B} \frac{dk k^4}{\sqrt{{M_B^*}^2 + k^2}} \\ &+ \frac{1}{3\pi^2}\sum_l \int_0^{k_l} \frac{dk k^4}{\sqrt{{m_l^*}^2 + k^2}} \qquad (2.14) \end{aligned}$$

3 A Relativistic Effective Approach for Finite Size Baryons

Effective Lagrangians like the one in Eq.(2.1), describe the long range behaviour of nuclear forces. At short distances, i.e. high densities, the strong

repulsive component of the baryon-baryon interaction appears as a consequence of the internal structure of the particles. In turn, this short range repulsion can be assimilated to a simplified model where baryons are described as extended objects over a spherical volume of radius R, where R reflects the range of the core repulsion. Therefore the fraction of available space is reduced with respect to the case of point-like particles. A similar approach has been applied to study the phase transition of nuclear matter to the quark-gluon plasma [11, 12] and in heavy-ion collisions [13, 14].
In our method we extend the Van der Waals prescription to take into account the finite size of different kinds of baryons including hyperons, at any finite density. For this purpose we shall use the effective Lagrangian (2.1) valid for low densities, but the solutions arising from Eq. (2.5) will be normalized within the available space. Our approach is expected to be valid for densities such that the center of mass of baryons be at a distance greater than $2R$ apart. Otherwise the simple quasiparticle picture breaks down.
Thus we start from the plane wave solutions ψ of the Dirac equation (2.5) for fermions of spin projection $s = \pm 1/2$ carrying momentum $\vec{k}$, and normalized in a volume V

$$\psi^B_{\vec{k},s}(x) = V^{-1/2} u^B(\vec{k}, s) e^{-ik^\mu x_\mu} \tag{3.1}$$

where $u^B(\vec{k}, s)$ is the spinor free particle solution in k space [23]. An analogous expression holds for the antiparticle solution.
We further assume that if particles have a finite size, then Eq.(3.1) refers to the dynamics of its center of mass. Since extended hadrons are assumed not to overlap their motion is restricted to the available space V' defined as [11, 12]

$$V' = V - \sum_B N^B v_B \tag{3.2}$$

with N^B the total number of baryons of class B inside the volume V, and v_B is the effective volume per baryon of class B. Hence if we renormalize the particle (antiparticle) wave function replacing V' for V, the effective baryon fields Ψ read

$$\begin{aligned} \Psi^B(x) = (V')^{-1/2} \sum_{\vec{k},s} \quad [\quad & a^B(\vec{k}, s) u^B(\vec{k}, s) e^{-ik^\mu x_\mu} \\ + \quad & b^{B\dagger}(\vec{k}, s) v^B(\vec{k}, s) e^{\,ik^\mu x_\mu} \;] \end{aligned} \tag{3.3}$$

as a function of the Fock space operators a and b, for particle and antiparticle respectively. In this way the finite size of the baryons is automatically accounted for into the field dynamics.
It is interesting to note at this point that a more detailed analysis shows that when we have a mixture of different baryons, the excluded volume is not exactly the same for all species, but depend upon their respective sizes [16]. To simplify the discussions, in this paper we assume that the sizes of the baryons are similar for all the species considered (see table 1), and hence the excluded volume is, to a good approximation, the same for every particle. With respect to the effective volume per baryon v_B, this quantity is expected to be proportional to the actual baryon volume, i.e. for spherical volumes of radius R_B

$$v_B = \alpha \frac{4\pi}{3} {R_B}^3 \tag{3.4}$$

and for sharp rigid spheres α is a real number ranging from 4, in the low density limit, to $3\sqrt{2}/\pi$, which corresponds to the maximum density allowed for non overlapping spheres, in a face centered cubic arrange. Since we wish to apply our method to study the high density behaviour of homogeneous isotropic matter, we shall adopt $\alpha = 3\sqrt{2}/\pi$ in all our calculations. Thus $v_B = 4\sqrt{2}{R_B}^3$ and the upper limit for the baryon density is given by $1/v_{max} = \sqrt{2}/(8{R_{max}}^3)$, where R_{max} denotes the biggest radius among all present baryonic classes.
In order to see how volume corrections appear in our approach, we shall use the renormalized field (3.3) to calculate the relationship between baryon densities n^B and the Fermi momenta k_B

$$n^B = V^{-1}\int_V dx^3 < GS|{\Psi^\dagger}^B\Psi^B|GS >= (1 - \sum_{B'} n^{B'} v_{B'})\ \frac{{k_B}^3}{3\pi^2} \tag{3.5}$$

where $\sum\limits_{\vec{k}} \to V'/(2\pi^3)\int dk^3$ has been used.
This result is equivalent to Eq. (2.8), if the factor ϑ takes now the value

$$\vartheta = 1 - \sum_B n^B v_B \tag{3.6}$$

for the case of finite baryon effective volumes v_B . In the limit $v_B \to 0$ one recovers the point-like expressions.
Thus we can still use the same expressions we have calculated in section 2.1 with ϑ satisfying Eq. (3.6)
Equation (3.5) shows that volume correlations couples non linearly the baryons among themselves, in a density dependent way.
We can solve explicitly Eq. (3.5) for n_B as a function of all the Fermi momenta k_B, namely

$$n^B = \frac{1}{(1 + \sum\limits_{B'} \frac{{k_{B'}}^3}{3\pi^2}\ v_{B'})}\ \frac{{k_B}^3}{3\pi^2} \tag{3.7}$$

Since ϑ in our approach depends explicitly upon the baryonic densities, the chemical potentials get an extra term, i.e.

$$\mu^B \ = \ \left(\frac{\partial\epsilon}{\partial n_B}\right)_{\substack{n_{B'} \\ B'\neq B}} = \mu_0^B + \Delta\mu^B \tag{3.8}$$

where $\mu_0^B = k_0^B(k_B)$, Eq. (2.6), is the free quasiparticle eigenvalue and

$$\Delta\mu^B = \frac{v_B}{3\pi^2}\sum_{B'}\int_0^{k_{B'}} \frac{dkk^4}{\sqrt{{M_{B'}}^{*2} + k^2}} \tag{3.9}$$

This value for $\Delta\mu^B$ is in agreement with the one used in the literature [11] - [14].
The expression for the energy density ϵ is formally the same given in (2.13), and the total pressure p adquires an additional term Δp

$$p = p_0 + \Delta p = p_0 + \sum_B n^B\Delta\mu^B \tag{3.10}$$

where p_0 is defined in Eq. (2.14), and ϑ is evaluated according to Eq. (3.6) in all the expressions.

In our approach only the baryonic states receive an explicit correction due to short range forces, through the normalization of the fields Ψ^B. This can be justified because meson fields contribute only through their mean values, which are completely determined from the baryonic sources. These sources already include finite size corrections in ϑ. Leptons do not experiment strong interactions, and in this sense they are taken as point-like particles. To resume, in our approach to finite volume correlations, matter properties are determined applying the set of equations (2.2) to (2.13), together with (3.8)-(3.10) for a fixed value of the total baryon density n, but using the value of ϑ given in (3.6) instead.

4 Effective Baryonic Models

4.1 The Zimanyi-Moszkowski Model

In order to have definite predictions of finite size effects we apply the scheme described in section 3, to the ZM model [20]. This is a local field model which basic degrees of freedom are point-like hadrons. This model has been extensively used to study nuclear matter and nuclei properties. It has the advantage of reproduce the main nuclear matter properties in the lowest order of approximation with reasonable accuracy, and using the minimum set of free parameters. In the ZM model, properly generalized to include several baryonic species, the effective baryon mass ${M_B}^*$ and its derivative $d{M_B}^*/d\sigma$ are given by

$$\begin{aligned} {M_B}^* &= M_B(1+g_\sigma^B\sigma/M_B)^{-1}, \\ \frac{d{M_B}^*}{d\sigma} &= -g_\sigma^B(1+g_\sigma^B\sigma/M_B)^{-2} \end{aligned} \tag{4.1.1}$$

respectively.
We place this expression for ${M_B}^*$ in the equations of sections 2 and 3, to calculate the effects of finite size corrections in the thermodinamical bulk properties.
If we take $\vartheta = 1$, section 2, we describe a system of point-like baryons, and using ϑ from Eq. (3.6), we include finite size effects. In the last case a fictitious volume of constant radius is assigned to each kind of baryons in order to contrast excluded volume effects with the point-like case. However, the high density results must be taken with caution since causality violation is expected due to the hard-core repulsion [13]. This problem can be avoided if the baryon volume decreases with density as predicted by the model presented in the next subsection.
Numerical results will be given in section 5.

4.2 The Quark Meson Coupling Model

Another baryon model we shall use is the Quark-Meson Coupling (QMC) model [8, 9]. The QMC model may be viewed as an extension of the Quantum Hadro-Dynamics (QHD) models like, for instance, the Walecka [21, 22] or the Zimanyi-Moszkowski [20] models. In the QMC model hadrons are represented as non-overlapping bags containing three valence quarks, the bag radius changing dinamically with the medium density. Baryons are interacting by the exchange of σ and ω mesons that couples directly to the confined quarks. It has been found that these extra degrees of freedom provided by the internal structure of the baryon lead to quite acceptable values of the nuclear matter compressibility at saturation. Despite the explicit quark fields present in the QMC model, hadronic thermodynamical properties are evaluated in such a way that baryons are handled as point-like particles with an effective mass M_B^* which depends on the σ field.
To describe briefly the QMC model, one considers baryons as spherical MIT bags where quarks are confined, the Dirac equation for a quark of flavor q, $(q = u, d, s)$, of current mass m_q and I_3^q third isospin component is then given by

$$(i\gamma^\mu\partial_\mu - g_\omega^q\gamma^0\omega_0 - g_\rho^q I_3^q\,\gamma^0 b_0 - {m_q}^*)\Psi^q = 0 \tag{4.2.1}$$

In this equation all meson fields have been replaced by their respective mean field values, in a similar way as we have done in Eq.(2.5) for baryons in uniform hadronic matter. Mesons are supposed to couple linearly only to u and d quarks, i.e. $g_\sigma^s = g_\omega^s = g_\rho^s = 0$. Therefore the effective ${m_q}^*$ masses are

$$\begin{aligned} {m_{u,d}}^* &= m_{u,d} - g_\sigma^{u,d}\sigma \\ {m_s}^* &= m_s \end{aligned} \tag{4.2.2}$$

For a spherically symmetric bag of radius R_B, representing a baryon of class B, the normalized quark wave functions $\Psi_B^q(r,t)$ are given by

$$\Psi_B^q(r,t) = \mathcal{N}_B^{-1/2}\frac{e^{-i\varepsilon_{qB}t}}{\sqrt{4\pi}}\begin{pmatrix} j_0(x_{qB}\,r/R_B) \\ i\beta_{qB}\vec{\sigma}.\hat{r}\,j_1(x_{qB}\,r/R_B)\end{pmatrix}\chi^q \tag{4.2.3}$$

where χ^q is the quark spinor and

$$\varepsilon_q = \frac{\Omega_{qB}}{R_B} + g_\omega^q\,\omega_0 + g_\rho^q I_3^q\,b_0 \tag{4.2.4}$$

$$\mathcal{N}_B = {R_B}^3\,[2\Omega_{qB}(\Omega_{qB}-1) + R_B{m_q}^*]\,\frac{j_0^2(x_{qB})}{x_{qB}^2} \tag{4.2.5}$$

$$\beta_{qB} = \left[\frac{\Omega_{qB} - R_B{m_q}^*}{\Omega_{qB} + R_B{m_q}^*}\right]^{1/2} \tag{4.2.6}$$

with $\Omega_{qB} = [x_{qB}^2 + (R_B{m_q}^*)^2]^{1/2}$. The eigenvalue x_{qB} is solution of the equation

$$j_0(x_{qB}) = \beta_q\,j_1(x_{qB}) \tag{4.2.7}$$

which arises from the boundary condition at the surface of the bag.
In this model the ground state bag energy is identified with the baryon mass ${M_B}^*$,

$${M_B}^* = \frac{\sum_q n_q^B\Omega_{qB} - z_{0B}}{R_B} + \frac{4}{3}\pi B_0{R_B}^3 \tag{4.2.8}$$

where n_q^B is the number of quarks of flavor q inside the bag, $B_0^{1/4} = 210.85MeV$ is the bag constant and z_{0B} the zero-point motion parameter, fixed to reproduce the baryon spectrum at zero density.

baryon	$M(MeV/c^2)$	$R(fm)$	z_0
p	938.2723	0.6	4.00496464
n	939.5656	0.6	4.00102120
Λ	1115.63	0.606	3.86577814

Table 1: Baryon parameters. M and R are, respectively, the mass and the radius at zero density. For the ZM model R is density independent. The bag constant B_0 has been fixed by the value $B^{1/4} = 210.8MeV$.

To obtain this mass one has first to solve Eq. (4.2.7), with (4.2.2) and the σ_0 mean field given by (2.2) where the derivative in this equation must be interpreted as $(\partial M_B^*/\partial\sigma)_R$.
Equation (4.2.8) shows that the baryon effective mass is a function of the bag radius R_B. In the original MIT bag calculations R_B is a constant fixed at zero baryon density, but in the QMC it is a variable dynamically adjusted to reach the equilibrium of the bag in the dense hadronic medium. We shall consider two possibles equilibrium conditions, to be combined with the point-like and finite size considerations. They are:

a) the standard QMC prescription which minimizes ${M_B}^*$ with respect to R_B keeping the σ field constant, namely [9]

$$\left(\frac{\partial {M_B}^*}{\partial R_B}\right)_\sigma = 0 \tag{4.2.9}$$

This prescription will be denoted as $QMCa$.

b) an alternative version of the QMC model, more suitable to account for the bag equilibrium at high pressures, is obtained by impossing that the net momentum flux through the bag surface be zero [24] (see Appendix)

$$-\left(\frac{\partial {M_B}^*}{\partial v_B}\right)_{\sigma,x_{qB}} = \frac{1}{3\pi^2}\sum_{B'}\int_0^{k_{B'}} \frac{dkk^4}{\sqrt{{M_{B'}}^{*2}+k^2}} \tag{4.2.10}$$

where the left hand side is the pressure exerted by the quarks inside the bag of kind B and the right hand side is the baryon contribution to the total hadronic pressure.
This condition will be labelled as $QMCb$ in what follows.

It must be mentioned that a similar condition can be obtained by minimizing the energy density ϵ with respect to the effective bag volume v_B, keeping constant the total volume V, namely [11, 12]

$$-\frac{n_s^B}{n^B}\left(\frac{\partial {M_B}^*}{\partial v_B}\right)_{\sigma,x_{qB}} = \frac{1}{3\pi^2}\sum_{B'}\int_0^{k_{B'}} \frac{dkk^4}{\sqrt{{M_{B'}}^{*2}+k^2}} \tag{4.2.11}$$

The only difference with Eq.(4.2.10) stands in the factor n_s^B/n^B. This factor is found numerically to be close to unity in the range of densities we handle

in the present work. In fact, numerical results using condition (4.2.11) differ only by negligible amounts with respect to the predictions arising from (4.2.10) for symmetric nuclear matter.
Hence we prefer to use the much simpler condition (4.2.10) for further calculations.

Conditions $QMCa$ and $QMCb$ coincide only in the case of vanishing density, but the last one seems to be more appropriate to describe general equilibrium situations of bags inmersed in high density medium.

Once $M_B{}^*$ has been defined microscopically, the dynamics of the hadrons in the QMC model arises from the effective Lagrangian (2.1), as discussed in section 2.
Only the couplings of mesons to baryons remains to be properly defined, since in this model mesons interacts directly with quarks. In fact, the quark-meson couplings g^q_ϕ, with $\phi = \sigma, \omega, \rho$ and $q = u, d$, are related to the corresponding meson-baryon couplings in a simple way [9]. If we denote with g^B_ϕ the coupling of the ϕ-meson to B-baryon, and calling n^B_{ns} the non-strange quark content of baryon B, then

$$\begin{aligned} g^B_\sigma &= \frac{n^B_{ns}}{3} g^u_\sigma \\ g^B_\omega &= \frac{n^B_{ns}}{3} g^u_\omega \\ g^B_\rho &= g^u_\rho \end{aligned} \tag{4.2.12}$$

When $\vartheta = 1$ (see section 2), we neglect the particle size in the evaluation of many-body effects. Otherwise these are included using Eq.(3.6) for ϑ instead.
An interesting fact related to the QMC model is that the bag volume reflects the changes in the medium density through the mean value of the σ field appearing in either of the equilibrium conditions $QMCa$ or $QMCb$. This is a self-consistency condition since σ itself depends on the effective volume of the baryons through the coefficient ϑ.
Numerical results will be discussed in the next section.

Model	Case	g_σ	g_ω	g_ρ	g^Λ_σ	g^Λ_ω
ZM	NC	7.8449	6.6710	9.4802	4.6760	4.9620
	VC	7.4039	5.8275	9.2446	4.1997	4.2872
$QMCa$	NC	17.964	9.012	9.220	11.977	6.008
	VC	17.007	8.172	8.873	11.338	5.448
$QMCb$	NC	17.985	9.024	9.219	11.990	6.016
	VC	17.046	8.199	8.870	11.364	5.466

Table 2: Baryon-meson couplings $g_{\sigma,\omega,\rho}$ used in our calculations, for the ZM, $QMCa$ and $QMCb$ models as described in the text, and combined with the point-like (NC) and finite size (VC) cases. The couplings has been adjusted in order to reproduce the symmetric nuclear matter properties at saturation in either case, see section 5.1.

5 Finite size effects: Numerical Results

5.1 Homogeneous symmetric nuclear matter

Nuclear matter properties has been extensively studied using point-like hadronic models. We wish to investigate excluded volume corrections in the homogeneous symmetric nuclear matter equation of state (EOS). With this purpose we shall use alternatively the hadronic models ZM and QMC to apply the scheme described in section 3. Physical predictions for point-like ($\vartheta = 1$) and finite extension baryons will be compared, and for the QMC case we also have considered two alternative conditions for the equilibrium of bags in the nuclear medium. In the following we shall use the labels VC and NC to indicate results obtained with or without excluded volume correction, respectively. Also the labels a and b will be associated with the QMC model to distinguish between the proposed equilibrium conditions, as explained in the previous section.

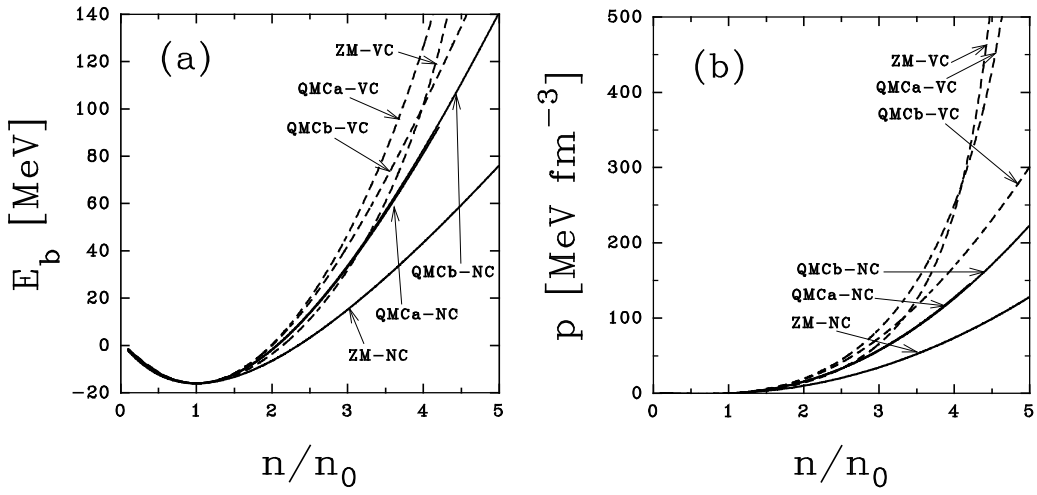

Figure 1: Thermodynamical properties of symmetric nuclear matter: binding energy $E_b = (\epsilon/n) - \bar{M}c^2$ (a) and pressure (b) as functions of the relative baryon density. The curves corresponds to the models Zimanyi-Moszkowski (ZM) and Quark-Meson Coupling (QMC). Results with excluded volume correction (VC) are represented with dashed lines and those without this correction (NC) by solid lines. For the QMC model the cases $QMCa$ and $QMCb$ arise by selecting different equilibrium conditions as explained in the text.

The equations to be solved for nuclear matter are the same as those in the neutral matter case described in section 2, except that proton and neutron densities are equal ($n^p = n^n$), hyperons and leptons are absent and hence Eq.(2.11) for electrical neutrality no longer holds.
In tables 1 and 2 we display the set of parameters to be used in both the ZM and QMC models, respectively, combined with different possibilities, as explained in the table captions. Each set of parameters has been obtained with the constraint that the known symmetric nuclear matter properties at saturation must be reproduced, i.e. the saturation density n_0, the binding energy per nucleon E_{b0}, and the symmetry energy coefficient a_s:

$$n_0 = \ 0.15 fm^{-3}$$
$$E_{b0} = (\epsilon/n)_0 - \bar{M}c^2 = -16 MeV$$

$$a_s = \frac{1}{2}\left(\frac{\partial^2(\epsilon/n)}{\partial t^2}\right)_{t=0} = 35MeV \qquad (5.1.1)$$

where $n = (n_n + n_p)$ is the total nucleon density, $t = (n_n - n_p)/n$ and $\bar{M} = 938.92MeV/c^2$ is the average free nucleon rest mass.
When finite size baryons are considered we fix the nucleon radius in vaccum at $0.6fm$; with this choise the upper nuclear density allowed for non overlapping bags is always beyond $n/n_0 = 5$, for the set of parameters in tables 1 and 2.
In figure 1a we plot the binding energy $E_b = (\epsilon/n) - \bar{M}c^2$, as function of the relative baryon density n/n_0 up to 5 times the saturation density, for both ZM and QMC models, with and without finite volume corrections. Also we show in figure 1b the total pressure for symmetric nuclear matter, corresponding to the same cases depicted in figure 1a. We can see in either figures 1a and 1b that all the cases practically coincide in the range $0 < n/n_0 < 1.5$. Thus, as expected, in this density domain the short range nucleon-nucleon repulsion can be neglected.
In particular the nuclear matter compressibility at saturation, $\kappa = 9(\partial p/\partial n)_{n_0}$, is only slightly increased by finite volume corrections, the increment is about 15% in the ZM and about 8% in the QMC models, see table 3.

Model	Case	$M_p{}^*/M_p$	κ (MeV)
ZM	NC	0.850	221.4
	VC	0.862	254.1
$QMCa$	NC	0.773	300.6
	VC	0.792	323.4
$QMCb$	NC	0.772	296.1
	VC	0.791	318.6

Table 3: Predicted properties for symmetric nuclear matter at saturation, using the ZM and QMC models with the corresponding set of couplings constants detailed in Table 2.

For the QMC formalism the cases a and b are practically undistinguishable when volume corrections are not included, meanwhile in the VC approach there are significative differences only for densities higher than $2.5n_0$. For every case the inclusion of the proposed corrections enhances, for a given density, both pressure and binding energy. This increment is greater for $QMCa$ than for $QMCb$. This behaviour can be explained by looking at figure 2a, where we plot the density dependence of the proton radius R_p. In fact, one sees there that all predictions are very similar for densities below n_0, but at higher densities the bag size decreases much faster in the option $QMCb$ including or not volume corrections, as compared with the option $QMCa$ and therefore in the option $QMCb$ ϑ is always closer to unity. The behaviour shown in figure 2a could be expected because in the condition $QMCb$ the bag must support the growing external baryon pressure, while option $QMCa$ only equilibrates the in-medium bag with its internal structure.
To conclude, in case $QMCb$ the excluded volume remains negligible in a wider density range, allowing the baryonic system to compress to much higher

densities as compared with the standard option $QMCa$, or with the rigid, undeformable baryon used for the ZM model.
Also it must be noted in this figure that corrections effects have opposite signs in cases $QMCa$ and $QMCb$.
The pronounced compression of the bags predicted by the $QMCb$ case could justify the use of effective point-like equations to extrapolate thermodynamical bulk properties at high densities, provided the bag compression is appropriately accounted for in the effective baryon mass.

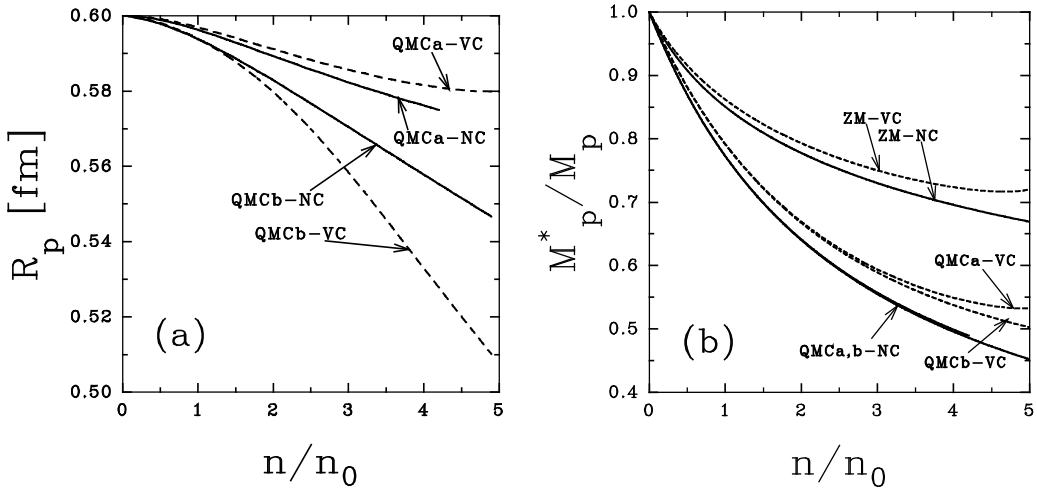

Figure 2: Properties of nucleon immersed in symmetric nuclear matter: the proton radius (a) and the proton mass (b) as functions of the relative baryon density. In the first case only QMC results are shown since in the modified ZM model a constant radius is assumed for all the baryons. The lines and labels conventions are the same as those defined in fig. 1.

In figure 2b we plot the behaviour of the proton effective mass M_p^*/M_p as function of the relative nucleon density. This figure shows that repulsive finite size effects tends to stabilize the effective mass when the density increases, for both the ZM and QMC models.
On the other hand the difference between equilibrium conditions $QMCa$ and $QMCb$ becomes significative for the effective mass only for extremely high densities.

5.2 Homogeneous neutral matter

We proceed to calculate numerically the effects of finite baryonic size on neutral matter properties, using alternatively the ZM and QMC models. The parameters inherent to each model have been fixed in the previous section, tables 1 and 2.

To simplify the discussion, we study hyperon neutral matter compossed only by protons, neutrons and lambdas, together with electrons and muons. In the ZM case the coupling of the hyperon Λ to mesons must be determined from experimental data. We use the condition that the binding energy of a single Λ in symmetric nuclear matter must have a minimum of $-28MeV$ [25] at the saturation density n_0. This condition determines the values $g^{\Lambda}_{\sigma,\omega}$, which

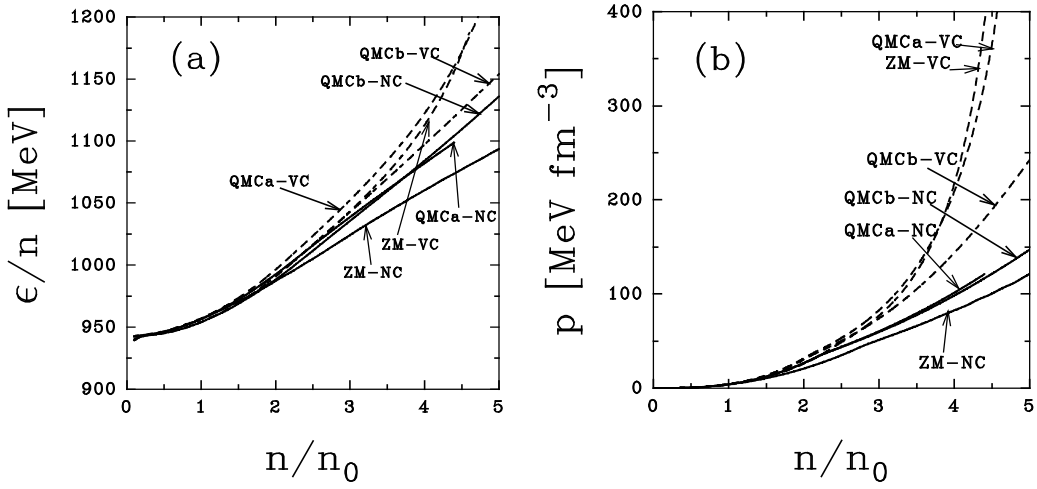

Figure 3: Thermodynamical properties of electrically neutral nuclear matter with Λ hyperons in β equilibrium with leptons: the energy per particle (a) and the pressure (b) as functions of the relative baryon density. The lines and labels conventions are the same as those in fig. 1.

are quoted in table 2, for the NC and VC cases. In the QMC framework the Λ coupling constants are reduced to 2/3 of the value corresponding to non-strange nucleons; numerical values of $g^{\Lambda}_{\sigma,\omega}$ are quoted in table 2.

In figures 3a and 3b the relativistic energy per baryon ϵ/n and the pressure p are drawn versus the relative baryon density, respectively. Most of the general conclusions given for nuclear matter can be repeated here: the VC approach increases, for a given density both pressure and energy, independently of the model used.

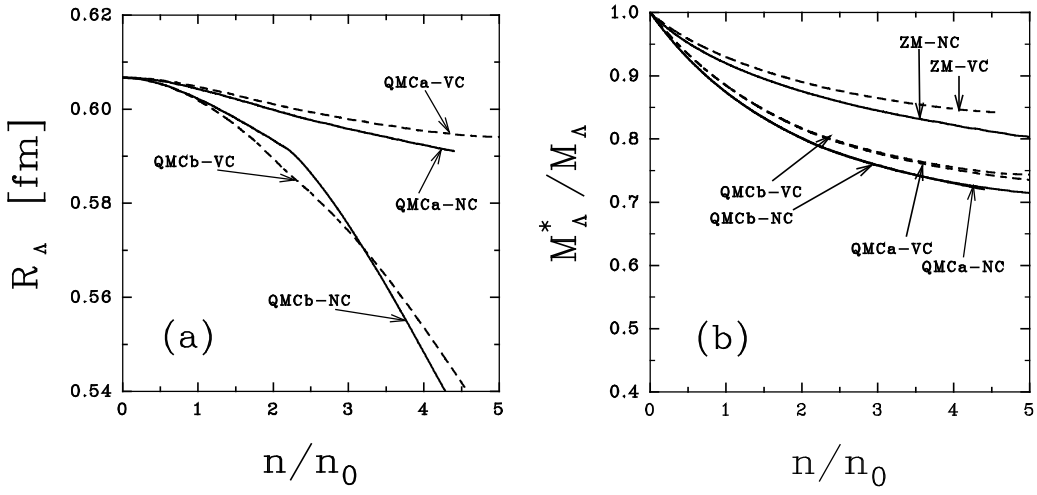

Figure 4: Properties of the Λ in neutral nuclear matter in β equilibrium: the bag radius (a) and the effective mass (b) are shown as functions of the relative baryon density. In the first case only QMC results are displayed. The lines and labels conventions are the same as those in fig. 1.

The effects of this correction are more significative for ZM and $QMCa$ and less important for $QMCb$.

The density dependence of the raddii and effective masses of nucleons are

very similar to the result obtained for symmetric nuclear matter. The behaviour of R_Λ with the density is depicted in figure 4a for the QMC model, and the density dependence of the Λ mass appears in figure 4b; it can be seen that finite volume corrections enhance this effective mass for all the cases considered, stabilizing its high density behaviour.
An interesting aspect of the volume effects arises in the relative baryonic populations, n_B/n, and leptonic populations, n_l/n, as a function of the baryon density, figures 5a and 5b. In figure 5a we study the change in the relative particle populations for the ZM model, one can see that the finite volume correlations enhance the production of hyperons as compared with the point-like case. Furthermore the Λ particles appear at a relative density of 2.5 (thin medium-dashed line), a bit earlier than in the point-like description (thick medium-dashed line). This could be expected since at high densities the finite size correlations favours the creation of heavier electrically neutral particles, decreasing the pressure of the system. This last statement proves to be true provided the size of the hyperon is similar to the size of the nucleons, as occurs in the present case.
In figure 5b we plot the relative particle population for the $QMCb$ treatment, a qualitative agreement with this figure is obtained when the stability condition $QMCa$ is used. It can be seen that in the QMC model the inclusion of finite volume correlations modifies very little the relative presence of the hyperon Λ, which appears at lower densities with respect to the predictions of the ZM model.
These results can be also compared with those obtained in ref.[26], where baryons are considered as point-like.

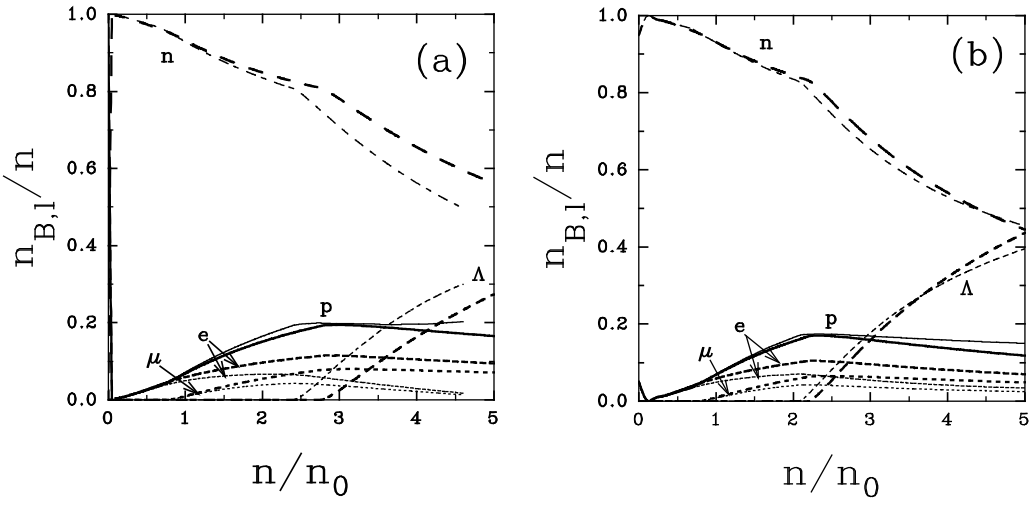

Figure 5: Relative populations of baryons and leptons as functions of the relative baryon density for the modified ZM model (a) and the QMC model (b). In the last case only results for the equilibrium condition $QMCb$ are shown. Different line types are used for each particle. For each class of particle thick (thin) lines represents NC (VC) calculations.

6 Conclusions

We have introduced finite size volume correlations to extend the study of matter properties at densities much higher than that of symmetric nuclear

matter at the saturation point. This has been performed through a Van der Waals approach to describe hypermatter at zero temperature. One of the advantages of the present approach consists in that we can continue to use the relativistic effective Lagrangians appropriate for low baryonic density, because the excluded volume corrections appear within the normalization of the baryon fields.

We have choosen two effective models to compare the effects of finite volume correlations with respect to the more usual point-like descriptions, these are the ZM and the QMC models. First we have enlarged the range of applicability of Van der Waals volume correction to higher densities by introducing a model (QMC) that avoids causality violation [13]- [15], since the hard core has been replaced with a compressible bag structure. Second, although the QMC model deals with finite volume bags, this property is usually lost in the calculation of thermodynamical properties. This feature has been partially corrected in the results QMC-VC of this work.

Near the normal saturation density finite volume effects prove to be small for both the ZM and the QMC models. At higher densities these repulsive short range effects show up in a model dependent way. For the ZM model with rigid hadrons, the pressure and the energy raise steeper than for the point-like prediction as the density gets closer to the touching limit. This favours the production of Λ hyperons in our example.

For the QMC model we have obtained that the contribution of finite effects depends significantly on the bag equilibrium condition used, as explained in the text. Using the standard condition the bags are not seriously compressed with density and volume corrections can be appreciable in the EOS but not in the change of relative particle occupation.

On the other side, if the bags must equilibrate the external baryonic pressure, a seemingly more physical condition, their respective radius suffer a faster reduction when the density increases. Therefore assuming the validity of this approach, short range correlations could be neglected in the EOS up to much higher densities, provided the compression effects are included in the baryonic effective mass as the QMC model does. In fact those physical aspects related to the size of the hadrons itself will be seriously affected by the choise of the equilibrium conditions.

A general conclusion is that finite volume corrections are less significative in the EOS when the medium density influence on the hadron structure is properly taken into account inside the model prescriptions.

The production of hyperons is sensibly affected by excluded volume correlations, decreasing its density threshold and enhancing its relative population as density increases.

This studies on finite baryonic size effects on hyperon matter properties aim to describe more properly the possible composition and structure of neutron stars. However a more complete treatment must include the full baryon octet.

Appendix

In order to deduce the equilibrium condition proposed for case $QMCb$ we consider only σ and ω mesons. The inclusion of other mesons is straigthforward. The QMC lagrangian density with quark fields $\Psi_q(x)$ coupled to scalar $\sigma(x)$ and vector $\omega_\mu(x)$ neutral mesons, is written as follows

$$\mathcal{L}_{QMC}(x) = \sum_{q=1}^{3} \mathcal{L}_q(x) + \mathcal{L}^0_{Mesons}(x) \ , \tag{A.1}$$

$$\mathcal{L}_q(x) = \left(\mathcal{L}^0_q(x) - B\right)\Theta_V - \tfrac{1}{2}\bar{\Psi}_q(x)\Psi_q(x)\Delta_S \ , \tag{A.2}$$

Here Θ_V is the radial step function which schematically confine the quarks inside the spherical bag. The terms proportional to the surface delta function Δ_S ensures a zero net flux of quark current through the bag surface. In this lagrangian we have defined the following terms:

$$\begin{aligned}
\mathcal{L}^0_q(x) &= \bar{\Psi}_q(x)\left(i\gamma^\mu\partial_\mu - m_q + g^q_\sigma\sigma(x) - g^q_\omega\gamma^\mu\omega_\mu(x)\right)\Psi_q(x), \\
\mathcal{L}^0_{Mesons}(x) &= \frac{1}{2}[\partial^\mu\sigma(x)\partial_\mu\sigma(x) - m^2_\sigma\sigma^2(x)] - \frac{1}{4}F^{\mu\nu}(x)F_{\mu\nu}(x) \\
&\quad + \frac{1}{2}m^2_\omega\omega^\mu(x)\omega_\mu(x)
\end{aligned}$$

From this lagrangian the equations of motion of quarks and mesons can be derived

$$\Theta_V(i\ \partial\!\!\!/ - m_q + g^q_\sigma\sigma - g^q_\omega\ \omega\!\!\!/)\Psi_q(x) = 0, \tag{A.3}$$

$$(\Box + m^2_\sigma)\sigma = \sum_{q=1}^{3} g^q_\sigma\bar{\Psi}_q\Psi_q\ \Theta_V, \tag{A.4}$$

$$\partial_\mu F^{\mu\nu} + m^2_\omega\omega^\nu = \sum_{q=1}^{3} g^q_\omega\bar{\Psi}_q\gamma^\nu\Psi_q\ \Theta_V, \tag{A.5}$$

these equations must be completed with the boundary conditions at the bag surface for the quark fields : $i\gamma\cdot\mathbf{n}\Psi_q(r=R) = \Psi_q(r=R)$ and $i\bar{\Psi}_q(r=R) = \bar{\Psi}_q(r=R)\gamma\cdot\mathbf{n}$.

In the following equations summation over quark-flavor indices is assumed.

The energy-momentum tensor is evaluated by the canonical procedure giving

$$T^{\mu\nu}_{QMC} = \frac{1}{2}i\Theta_V(\bar{\Psi}\gamma^\mu\overleftrightarrow{\partial^\nu}\Psi) + \partial^\mu\sigma\partial^\nu\sigma - F^{\mu\lambda}\partial^\nu\omega_\lambda - g^{\mu\nu}\mathcal{L} \tag{A.6}$$

inserting the explicit form of $\mathcal{L}$ and by taking its divergence one obtains

$$\begin{aligned}
\partial_\mu T^{\mu\nu}_{QMC} &= \frac{1}{2}i\Theta_V\partial_\mu(\bar{\Psi}_q\gamma^\mu\overleftrightarrow{\partial^\nu}\Psi_q) + \frac{1}{2}in_\mu\Delta_S(\bar{\Psi}_q\gamma^\mu\overleftrightarrow{\partial^\nu}\Psi_q) + \frac{1}{2}\partial^\nu(\bar{\Psi}_q\Psi_q\Delta_S) \\
&\quad -\Theta_V\partial^\nu[\frac{1}{2}i\bar{\Psi}_q\overleftrightarrow{\partial\!\!\!/}\Psi_q + \bar{\Psi}_q(-m_q + g^q_\sigma\sigma - g^q_\omega\ \omega\!\!\!/)\Psi_q] \\
&\quad +Bn^\nu\Delta_S - [\frac{1}{2}i\bar{\Psi}_q\overleftrightarrow{\partial\!\!\!/}\Psi_q + \bar{\Psi}_q(-m_q + g^q_\sigma\sigma - g^q_\omega\ \omega\!\!\!/)\Psi_q]n^\nu\Delta_S \\
&\quad -\partial_\mu F^{\mu\lambda}\partial^\nu\omega_\lambda + \Box\sigma\partial^\nu\sigma + \frac{1}{2}\partial^\nu[m^2_\sigma\sigma^2 + m^2_\omega\omega_\lambda\partial^\nu\omega^\lambda]\,,
\end{aligned} \tag{A.7}$$

Using the equations of motion and rearranging terms one gets

$$\begin{aligned}\partial_\mu T^{\mu\nu}_{QMC} = &-\Theta_V \bar{\Psi}_q \partial^\nu (g^q_\sigma \sigma - g^q_\omega \not{\omega}) \Psi + \tfrac{1}{2} i \Delta_S n_\mu (\bar{\Psi}_q \gamma^\mu \overleftrightarrow{\partial^\nu} \Psi) + \tfrac{1}{2} \partial^\nu (\bar{\Psi}_q \Psi_q \Delta_S) \\ &-[\tfrac{1}{2} i \bar{\Psi}_q \overleftrightarrow{\not{\partial}} \Psi_q + \bar{\Psi}_q (-m_q + g^q_\sigma \sigma - g^q_\omega \not{\omega}) \Psi_q] n^\nu \Delta_S \\ &+ B n^\nu \Delta_S + (\Box + m^2_\sigma) \sigma \, \partial^\nu \sigma - (\partial \mu F^{\mu\lambda} + m^2_\omega \omega^\lambda) \partial^\nu \omega_\lambda \end{aligned} \tag{A.8}$$

the two terms in the squared bracket are canceled by using (A.3). If we denote by $\tilde{\Theta}_V$ the radial step function complementary to Θ_V, introducing the separation $1 = \Theta_V + \tilde{\Theta}_V$ in the last line and reagrouping terms

$$\begin{aligned}\partial_\mu T^{\mu\nu}_{QMC} &= \Theta_V [(\Box + m^2_\sigma)\sigma - g^q_\sigma \bar{\Psi}_q \Psi_q] \partial^\nu \sigma \\ &\quad -\Theta_V [(\partial \mu F^{\mu\lambda} + m^2_\omega \omega^\lambda) - \bar{\Psi}_q g^q_\omega \gamma^\lambda \Psi_q] \partial^\nu \omega_\lambda + B n^\nu \Delta_S \\ &\quad + \frac{1}{2} \Delta_S [i n_\mu (\bar{\Psi}_q \gamma^\mu \overleftrightarrow{\partial^\nu} \Psi_q)] + \frac{1}{2} \partial^\nu (\bar{\Psi}_q \Psi_q \Delta_S) \\ &\quad + [(\Box + m^2_\sigma)\sigma \, \partial^\nu \sigma - (\partial \mu F^{\mu\lambda} + m^2_\omega \omega^\lambda) \partial^\nu \omega_\lambda] \tilde{\Theta}_V \ . \end{aligned} \tag{A.9}$$

The first two terms on the right hand side are identically zero by virtue of Eqs. (A.4) and (A.5) respectively, therefore it becomes

$$\begin{aligned}\partial_\mu T^{\mu\nu}_{QMC} &= \Delta_S (B n^\nu + \frac{1}{2} i n_\mu \bar{\Psi}_q \gamma^\mu \overleftrightarrow{\partial^\nu} \Psi_q) \\ &\quad + \frac{1}{2} \partial^\nu (\bar{\Psi}_q \Psi_q \Delta_S) + \partial_\mu T^{\mu\nu}_{Mesons} \tilde{\Theta}_V \end{aligned} \tag{A.10}$$

where

$$\partial_\mu T^{\mu\nu}_{Mesons} = (\Box + m^2_\sigma)\sigma \, \partial^\nu \sigma - (\partial \mu F^{\mu\lambda} + m^2_\omega \omega^\lambda) \partial^\nu \omega_\lambda \tag{A.11}$$

In this way we can rewrite the above expression as follows

$$n_\nu \partial_\mu T^{\mu\nu}_{QMC} = n_\nu \partial_\mu T^{\mu\nu}_{bag} + n_\nu \partial_\mu T^{\mu\nu}_{Mesons} \tilde{\Theta}_V \tag{A.12}$$

with

$$n_\nu \partial_\mu T^{\mu\nu}_{bag} = (-P_D + B)\Delta_S + \frac{1}{2} n \cdot \partial (\bar{\Psi}_q \Psi_q \Delta_S) \tag{A.13}$$

where $P_D = -1/2 n \cdot \partial (\bar{\Psi}_q \Psi_q)|_{surface}$ is the pressure exerted by the quarks on the bag surface. The standard QMC equilibrium condition can be derived by requiring to be zero the first term of Eq.(A.12). Particularly, for the QMC model the second term of this equation is strictly zero, which is due to the fact that in the QMC lagrangian there is a static bag surrounded by free mesons. As the baryon density increases this picture is not adequate, since at high densities the mesons are far from the free field approximation. Although mesons are in the whole space, i.e. outside as well as inside the bags, the $\tilde{\Theta}_V$ in Eq.(A.12) is coming from a cancellation of identical terms as it has been shown. The fact that mesons are also inside the bag is reflected on the baryon density dependence of m_q, x_q, R, the quark wave functions, etc.

On the other hand, from the effective Lagrangian 2.1 we have $T^{\mu\nu}_{hadron} = T^{\mu\nu}_{fm} + T^{\mu\nu}_0$, where $T^{\mu\nu}_{fm}$ comes from the free meson sector and $T^{\mu\nu}_0$ is the contribution from baryons coupled to mesons. Energy-momentum conservation

implies $\partial_\mu T^{\mu\nu}_{hadron} = 0$. Explicit evaluation shows that $\partial_\mu T^{\mu\nu}_{fm} = \partial_\mu T^{\mu\nu}_{Mesons}$. Consequently, in this limit the second term of Eq.(A.12) can be replaced by $-\partial_\mu T^{\mu\nu}_0$. Multiplying the resulting equation by n_ν and integrating on the external bag volume we obtain

$$4\pi R^2(-P_D + B) = \int dS n_\mu n_\nu T^{\mu\nu}_0 \,. \tag{A.14}$$

For homogeneous hadronic matter $T^{\mu\nu}_0$ can be assumed as constant on the bag surface, obtaining the following equation

$$-P_D + B = n_\mu n_\nu T^{\mu\nu}_0 (r = R) \tag{A.15}$$

where n_λ is a (space-like) radial unit vector. Therefore, we get

$$-P_D + B = \frac{1}{3}\sum_{i,j} T^{ij}_0 \tag{A.16}$$

In the case of homogeneous static matter the space sector of the relativistic energy-momentum tensor is diagonal [27], which implies that

$$-P_D + B = \frac{1}{3}\sum_{i}^{3} T^{ii}_0 = -P_0 \tag{A.17}$$

where P_0 is a pressure related to T_0. In this form we have obtained the equilibrium condition of case $QMCb$.

References

[1] H. Hatsuda and T. Kunihiro, Phys. Rep. **247** (1994) 221.

[2] G. E. Brown and M. Rho, Phys. Rep. **269** (1996) 333.

[3] J. Rafelski, B. Müller, Phys. Rev. Lett.**48** (1982) 1066;
J. Kapusta, A. Mekjian, Phys. Rev. D **33** (1986) 1304;
T. Matsui, B. Svetitsky, L. D. McLerran, Phys. Rev. D **34** (1986) 783,2047;
P. Koch, B. Müller, J. Rafelski, Phys. Rep. **142** (1986) 167.

[4] E. Witten, Phys. Rev. D **30** (1984) 272;
P. Haensel, J. L. Zdunik, R. Schaeffer, Astron. Astrophys. **160** (1986) 121;
C. Alcock, C. E. Farhi, A. Olinto, Ap. J. **310** (1986) 261.

[5] N. K. Glendenning, Phys. Rev. D **46** (1992) 1274.

[6] J. Kapusta, Phys. Rev. D **23** (1981) 2444.

[7] A. Rakhimov, M. M. Musakhanov, F. C. Khanna and U. Yakhshiev, Phys. Rev. C **58** (1998) 1738.

[8] P. A. M. Guichon, Phys. Lett. B **200** (1988) 235.

[9] K. Saito and A. W. Thomas, Phys. Lett. B **327** (1994) 9; Phys. Rev. C **51** (1995) 2757;
K. Tsushima, K. Saito and A. W. Thomas, Phys. Lett. B **411** (1997) 9;
K. Tsushima, K. Saito, J. Haidenbauer and A. W. Thomas, Nucl. Phys. A **630** (1998) 691.

[10] K. Saito, K. Tsushima and A. W. Thomas, LANL preprint *nucl-th/9901084*.

[11] S. Kagiyama, A. Nakamura, T. Omodaka, Z. Phys. C **53** (1992) 163; **56** (1992) 557.

[12] S. Kagiyama, A. Minaka, A. Nakamura, Prog. Theor. Phys. **89** (1993) 1227.

[13] D. H. Rischke, M. I. Gorenstein, H. Stöcker and W. Greiner, Z. Phys. C **51** (1991) 485.

[14] J. Cleymans and H. Satz, Z. Phys. C **57** (1993) 135;
J. Cleymans , M. I. Gorenstein, J. Stålnacke, E. Suhonen, Phys. Scripta **48** (1993) 277;
H. Kouno, K. Koide, T. Mitsumori, N. Noda, A. Hasegawa, M. Nakano, Prog. Theor. Phys. **96** (1996) 191;
G. D. Yen, M. I. Gorenstein, W. Greiner, S. N. Yang, Phys. Rev. C **56** (1997) 2210;
M. I. Gorenstein, H. Stöcker, G. D. Yen, S. N. Yang, W. Greiner, J. Phys. G **24** (1998) 1777.

[15] C. P. Singh, B. K. Patra, K. K. Singh, Phys. Lett. B **387** (1996) 680.

[16] M. I. Gorenstein, A. P. Kostyuk and Ya. D. Krivenko, LANL preprint *nucl-th/9906068*.

[17] H. J. Schulze, M. Baldo, U. Lombardo, J. Cugnon and A. Lejeune, Phys. Rev. C **57** (1998) 704.

[18] L. L. Zhang, H. Q. Song and R. K. Su, J. Phys. G **23** (1997) 557.

[19] J. Schaffner, C. B. Dover, A. Gal, C. Greiner and H. Stöcker, Phys. Rev. Lett. **71** (1993) 1328.

[20] J. Zimanyi and S. A. Moszkowski, Phys. Rev. C **42** (1990) 1416;
R. J. Lombard, S. Marcos, J.Mareš, Phys. Rev. C **51** (1995) 1784;
R.Aguirre, O.Civitarese, A.L.De Paoli, Nucl. Phys. A **597** (1996) 543.

[21] J. D. Walecka, Ann. Phys. **83** (1974) 491; Phys. Lett. B **59** (1975) 109.

[22] B. D. Serot and J. D. Walecka, Advan. Nucl. Phys **16** (1986) 1; Int. J. Mod. Phys. E **6** (1997) 515.

[23] C. Itzykson and J.B. Zuber, Quantum Field Theory (McGraw-Hill, New York, 1980).

[24] R. M. Aguirre and M. Schvellinger, Phys. Lett. B **400** (1997) 245;
R. M. Aguirre and M. Schvellinger, Phys. Lett. B **449** (1999) 161.

[25] D. J. Millener, C. D. Dover and A. Gal, Phys. Rev. C **38** (1988) 2700.

[26] N. K. Glendenning, F. Weber, S. A. Moszkowski, Phys. Rev. C **45** (1992) 844.

[27] L. D. Landau and E. M. Lifshitz, Fluid Mechanics, Pergamon Press 1959, chapter XV.